Energy Efficient Autonomous Solar Water Pumping System

M Shunmuga sankari[#1], E.Elakkia[#2], M.Indumathy[#3]

[#1]*Assistant Professor, TJS Engineering college ,Peruvoyal*
[#2]*Assistant Professor, TJS Engineering college ,Peruvoyal*
[#3]*Assistant Professor, TJS Engineering college ,Peruvoyal*

[1]shankusaran@gmail.com
[2]elakkia.elumalai@gmail.com
[3]indumathy55@gmail.com

***Abstract* -This paper proposes a new converter and inverter for autonomous operation of a solar water pumping system. This system uses a modified two inductor boost converter (TIBC) for supplying energy to a 3ϕ induction motor through a three phase voltage source inverter (VSI). The TIBC has high voltage gain and low input current ripple. In this paper it is further improved with the use of non isolated recovery snubber to improve its efficiency. The 3ϕ VSI uses space vector pulse width modulation technique (SVPWM) for producing pulses to control the MOSFET switches. By this technique the THD is reduced to 16.24% and the results are shown in MATLAB. As a result this system produces low torque ripple, low rise time and settling time for the induction motor operation and hence well suited for the operation of an autonomous solar water pump.**

Index terms

Ac motor drives, dc-ac power conversion, dc-dc power conversion, solar power generation , space vector pulse width modulation

I . INTRODUCTION

Renewable energy sources exist over wide geographical areas, in contrast to other energy sources which are concentrated in a limited number of countries[1][2][3]. Rapid development of renewable energy and energy sufficiency is resulting in significant energy security, climate change mitigation and economic benefits. National renewable energy markets are projected to continue to grow strongly in the coming decade and beyond.

In countries such as interior parts of brazil the unavailability of electric power supply to the people of that area ,the need for pumping becomes difficult as by conventional means, so PV based water pumping systems are becoming more efficient in pumping water to the community[4]

Till now the converters used in Brazil are based on an intermediate storage system, which uses lead acid batteries and dc motors to drive the water pump[6]. Now the use of low voltage synchronous motors have been developed which gives high efficiency, but they are very expensive to be used in poor communities.

The batteries make the motor to operate at its rated voltage. This makes the coupling of solar panel and the motor .The batteries used have a short life span compared to the average useful life of PV panel. further, the lack of battery replacement is another problem for such system to be used in isolated areas.

Many commercial systems use low voltage dc motors so that boost stage can be avoided between PV and motor. But dc motors have low efficiency and high maintenance cost as compared to the induction motor. Also low voltage dc motors are not easily available in markets. Because of this 3ϕ induction motors are used in pumping system.

The design of a motor drive system supplied directly from solar demands constant power to be supplied which creates a need for a converter with the following features. High efficiency due to low energy available, low cost, robustness ad autonomous operation.

This paper proposes a new dc/dc converter and a three phase VSI with space vector pulse width modulation control for the MOSFET switches. The paper is organised as follows. In section II the dc/dc converter is described. In section III the 3ϕ VSI is described and the section IV describes the simulation results obtained from MATLAB.

II. TIB CONVERTER

In a number of high power applications, the performance of boost converter is improved by implementing the boost converter with multiple switches and multiple boost inductors as shown in fig.1. This topology is usually employed in high power applications with a high input voltage or in applications where the conversion efficiency of a single switch boost topology is significantly degraded by the reverse recovery losses of the boost rectifier.

A two switch two inductor boost converter achieves output voltage regulation in a wide input and load current range using a constant frequency by employing an auxiliary transformer to couple current path of the two boost inductors so that both the inductors carry the same current. By forcing the current through the boost inductors to be the same the energy in both the inductors is forced to change simultaneously that is both the inductors increase the energy when both switches are turned on and simultaneously decrease energy when either of the converter two switches is turned off.

As a result the stored and transferred energy of both the inductors can be controlled in a wide input voltage and load range using a constant frequency control by

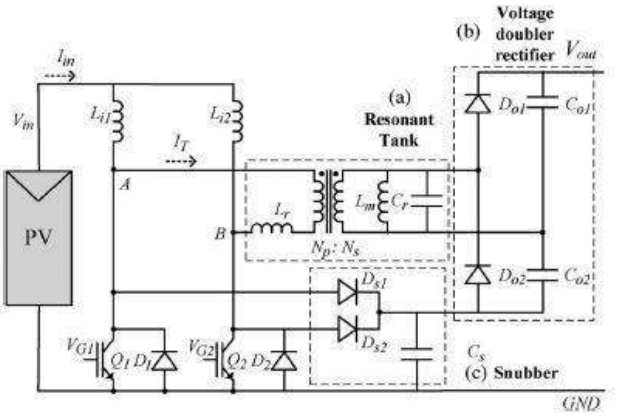

Fig.1.modified TIBC topology

controlling the time duration that the two switches are simultaneously on.

The TIBC must have a minimum operation load to maintain an established output voltage. Below a certain load level, the energy transferred to the output capacitor is not completely transferred to the load and causes an increase in the output voltage. This happens because of the inductors are charged even if there is no output current.

As a result, this converter has a drawback when used in motor drive system.As a solution for the drawback, a non dissipative regenerative snubber circuit is presented in the modified TIBC. The regenerative snubber is formed by two diodes and the capacitor connecting the input side directly to the output side of the converter[7] This makes it a non isolated converter which has no desirable effect in the PV motor driver applications

To solve the minimum load conditions , the use of a hysteresis controller for the dc output voltage of the first stage is proposed[8]. When operating below the minimum required load an uncontrolled increase of output voltage will be seen and once this voltage reaches the upper threshold, both primary switches are turned off. This should be impossible in all the previously reported implication of TIBC. However with an added snubber even with both switches turned off, there is still a path for the input inductors current. This energy is directly transferred to the snubber capacitor C_s.

Once the multi resonant tank is introduced, two different resonant processes occur 1) When both switches are closed, the leakage inductance L_r participates along with capacitance C_r in the resonance at the primary current switching and current polarity inversion and 2) during the conduction time interval when at least one of the switches is open, L_r is associated in series with L_{i1}, or L_{i2} not participating on the transformer's secondary current resonance, formed only by L_m and C_r.

At time t_1, the rectifying diode D_{o1} is already conducting, and the voltage on resonant capacitor C_r, is clamped at $V_{out}/2$. At this instant, the switch Q_1 is activated by V_{G1}. At the time t_2, the voltage V_{ds2} starts to increase, Q_2 is completely blocked, and the snubber diode D_{s2} begins to conduct, transferring energy directly to the snubber capacitor C_s. Between t_2 and t_3, C_r and L_m continue to resonate, decreasing the voltage on the doubler rectifier's input and on V_{Cr}. At instant t_3, the voltage across C_r reaches $-V_{out}/2$, and the rectifying diode D_{o2} starts to conduct, clamping V_{Cr} in $-V_{out}/2$.

From t_4 to t_5, the capacitor C_s is charged and the current of D_{s2} starts to decrease. At the instant t_5, Q_2 is turned on initiating the resonant process on Q_2. As Q_2 is activated, D_{s2} is forced to stop conduction. At the instant t_6, the current in D_{o2} reaches zero, and D_{o2} stops conducting re-initiating the resonance between C_r and L_m [9]. From this moment until the end of the switching period, the process repeats symmetrically as explained for the other input switch.

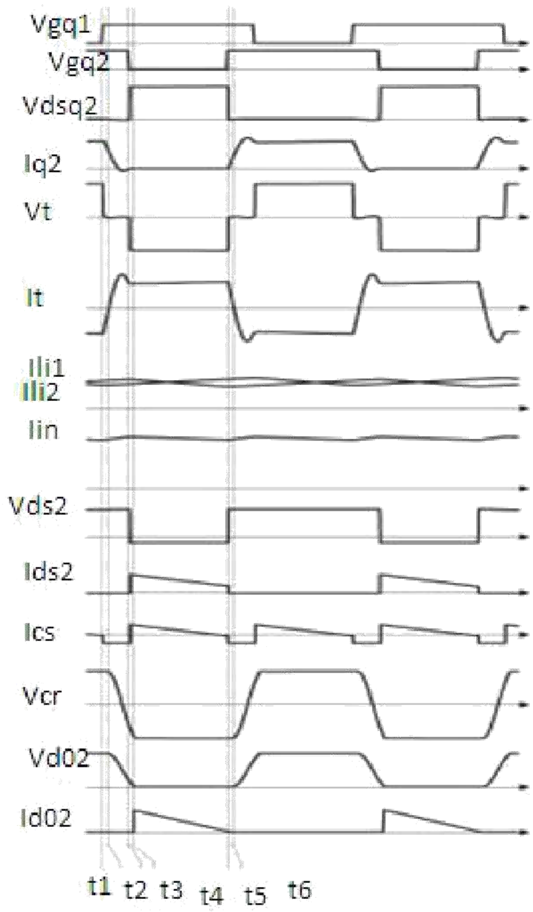

Fig.2. Waveforms for TIBC Operation

III. THREE PHASE VSI

The output voltage from modified two inductor boost converter is given to a 3φ voltage source inverter (VSI). The 3φ VSI consists of 6 MOSFET switches. The gate signals to the MOSFET are given by the Space Vector Pulse Width Modulation technique (SVPWM)[8]. The use of this PWM strategy is to improve the output voltage level as compared to sinusoidal pulse width modulation strategy with 1/6 optimal third harmonic voltage injection.

Vector	A^+	B^+	C^+	A^-	B^-	C^-	V_{AB}	V_{BC}	V_{CA}	
V_0 = {000}	OFF	OFF	OFF	ON	ON	ON	0	0	0	zero vector
V_1 = {100}	ON	OFF	OFF	OFF	ON	ON	$+V_{dc}$	0	$-V_{dc}$	active vector
V_2 = {110}	ON	ON	OFF	OFF	OFF	ON	0	$+V_{dc}$	$-V_{dc}$	active vector
V_3 = {010}	OFF	ON	OFF	ON	OFF	ON	$-V_{dc}$	$+V_{dc}$	0	active vector
V_4 = {011}	OFF	ON	ON	ON	OFF	OFF	$-V_{dc}$	0	$+V_{dc}$	active vector
V_5 = {001}	OFF	OFF	ON	ON	ON	OFF	0	$-V_{dc}$	$+V_{dc}$	active vector
V_6 = {101}	ON	OFF	ON	OFF	ON	OFF	$+V_{dc}$	$-V_{dc}$	0	active vector
V_7 = {111}	ON	ON	ON	OFF	OFF	OFF	0	0	0	zero vector

T a b l e . 1 . Switching Vector Table

SVPWM is an algorithm for the control of pulse width Modulation. It is used for the creation of alternating current waveforms most commonly used to drive three phase AC powered motor at varying speeds[9][10].

Now looking down the columns for active switching vectors $V_1 - V_6$ the output voltages vary as a pulsed sinusoid, with each leg offset by 120 degrees of base angle[11][12]. The desired three phase voltages at the output of the inverter could be represented by an equivalent vector V rotating in counter clockwise direction[13].The magnitude of this vector is related to the magnitude of the output voltage and the time this vector takes to complete one revolution is the same as the fundamental time period of the output .

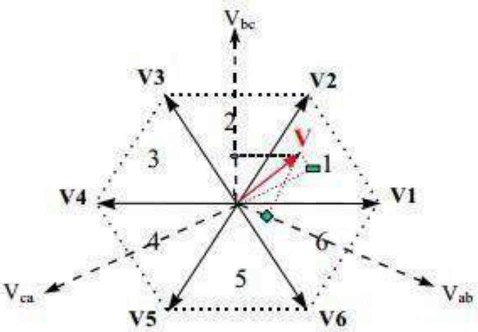

Fig.3.Output voltage vector in α,β plane

Let us consider the situation when the desired line to line output voltage vector V is in sector 1 This vector could be synthesized by the pulse with modulation of two adjacent state space vector's (SSV) V_1 and V_2, the duty cycle of each being d_1 ,d_2 respectively and the zero vector of duty cycle d_0.

$$d_1 V_1 + d_2 V_2 = V = mV_g e^{j\theta}$$

$$d_1 + d_2 + d_0 = 1$$

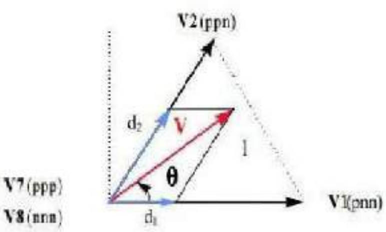

Fig.4. Synthesis of the Output Voltage Vector in Sector 1

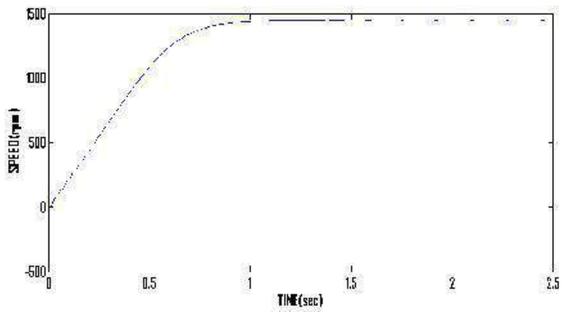

Fig.5. Speed Curve

Where $0 \le m \le 0.866$ is the modulation index[14]. This would correspond to a maximum line to line voltage of 1.0 vg which is 15% more than conventional sinusoidal plus $1/6^{th}$ optimal third harmonic injection PWM.

If this algorithm uses non adjacent SSV's then it will produce higher THD and switching loses. This output waveform for all the six sectors are shown in Fig 3.5. These six sectors together form a cycle of period Ts = 1/fs.

The THD of a periodic voltage which can be represented by the Fourier series

$$V = \sum_{n=1}^{\infty} V_n e^{-jn\omega t}$$

is defined as

$$THD = \sqrt{\sum_{n=2}^{\infty} V_n^2} / V_1$$

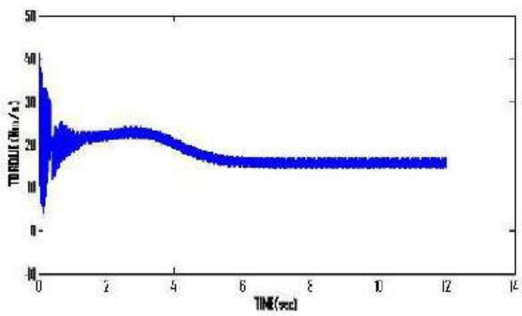

Fig.6.torque curve

IV. SIMULATION RESULTS

The space vector simulation circuit is generated using a rotating vector in the αβ plane .The voltage in the αβ plane is compared with a reference voltage and the PWM pulses are generated in the rotating reference plane[15].

The simulink circuit for space vector pulse width modulation is shown in fig.8. The speed and torque curves for space vector pulse width modulation is shown in fig.5,6 respectively.

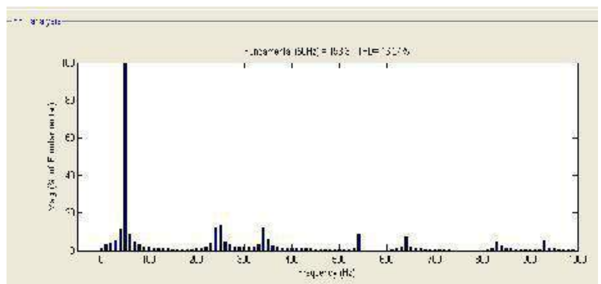

Fig.7.FFTanalysis

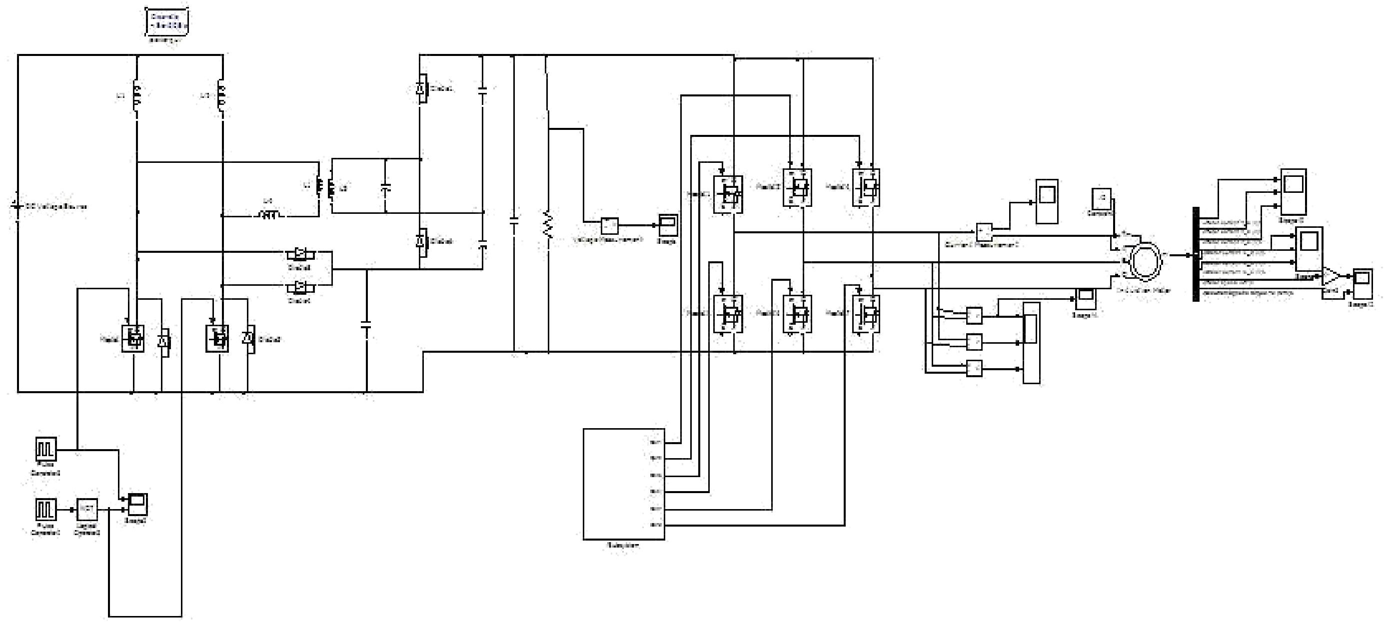

Fig.8.SVPWM simulation

V. CONCLUSION

From the adopted control method (SVPWM) and FFT analysis(fig.7) carried out the total harmonic distortion (THD) is reduced to 20% as compared to sinusoidal pulse width modulation with $1/6^{th}$ optimal third harmonic voltage injection method as is shown in table below. The induction motor performance is also improved. This work can be carried out with the soft computing techniques for giving pulses to the switches for better results.

	SPWM WITH 3^{RD} HARMONIC INJECTION	**SPACE VECTOR PWM**
THD	36.4%	16.4%
RISE TIME	4.2 sec	1.2 sec
SETTLING TIME	5.9 sec	1.3 sec
TORQUE RIPPLE	15%	11.76%

Table.2.comparison table

VI.REFERENCES

1.João Victor Mapurunga Caracas, Guilherme de Carvalho Farias, LuisFelipe Moreira Teixeira, Luiz Antonio de Souza Ribeiro "Implementation of a High-Efficiency, High-Lifetime, and Low-Cost Converter for an Autonomous Photovoltaic Water Pumping System" IEEE transactions on industry applications, vol. 50, no. 1

2.R. Faranda and S. Leva, "Energy comparison of MPPT techniques for PV systems," *WSEAS Trans. Power Syst.*, vol 3, no. 6, pp. 446–455, Jun. 2008

3. M. A. Vitorino and M. B. R. Correa, "High performance photovoltaic pumping system using induction motor," in *Proc. Brazilian Power Electron. Conf.*, 2009, pp. 797–804.

4. G. Teröde, K. Hameyer, and R. Belmans, "Sensorless control of a permanent magnet synchronous motor for PV-powered water pump systems using the extended Kalman filter," in *Proc. 9th Int. Conf. Elect. Mach. Drives*, 1999, pp. 366–370.

5. H. Harsono, "Photovoltaic water pump system," Ph.D. dissertation, Dept. Intell. Mech. Syst. Eng., Faculty Kochi Univ. Technol., Kochi, Japan, Aug. 2003
.

6. D. Linden, *Handbook of Batteries and Fuel Cells*. New York, NY, USA: McGraw-Hill, 1984.

7. D. Tschanz, H. Lovatt, A. Vezzini, and V. Perrenoud, "A multi-functional converter for a reduced cost, solar powered, water pump," in *Proc. IEEE ISIE*, 2010, pp. 568–572

8. M. Cacciato, A. Consoli, and V. Crisafulli, "A high voltage gain dc/dc converter for energy harvesting in single module photovoltaic applications," in *Proc. IEEE ISIE*, 2010, pp. 550–555.

10. P. Wolfs and Q. Li, "An analysis of a resonant half bridge dual converter operating in continuous and discontinuous modes," in *Proc. IEEE Power Electron. Spec. Conf.*, 2002, pp. 1313–1318.

11. T.-J. Liang, R.-Y. Chen, J.-F. Chen, and W.-J. Tzeng, "Buck-type currentfed push-pull converter with ZCS for high voltage applications," in *Proc. IEEE Region 10 Conf.*, 2007, pp. 1–4.

12. P. M. Barbosa and I. Barbi, "A new current-fed, isolated PWM dc-dc converter," *IEEE Trans. Power Electron.*, vol. 11, no. 3, pp. 431–438, May 1996.

13. R.-Y. Chen, T.-J. Liang, J.-F. Chen, R.-L. Lin, and K.-C. Tseng, "Study and implementation of a current-fed full-bridge boost dc-dc converter with zero-current switching for high-voltage applications," *IEEE Trans. Ind. Appl.*, vol. 44, no. 4, pp. 1218–1226, Jul./Aug. 2008.

14. J. Kim, H.-S. Song, and K. Nam, "Asymmetric duty control of a dualhalf- bridge dc/dc converter for single-phase distributed generators," *IEEE Trans. Power Electron.*, vol. 26, no. 3, pp. 973–982, Mar. 2011.

15. B. Liu, C. Liang, and S. Duan, "Design considerations and topology selection for dc-module-based building integrated photovoltaic system," in *Proc. 3rd IEEE Conf. ICIEA*, Jun. 3–5, 2008, pp. 1066–1070.

16. L. Yan and B. Lehman, "Isolated two-inductor boost converter with one magnetic core," in Proc. IEEE Appl. Power Electron. Conf. Expo., 2003, pp. 879–885.

17. Y. Jang, "Two-boost converter," U.S. Patent 6 239 584, May 29, 2001.

18. Q. Li and P. Wolfs, "The power loss optimization of a current fed ZVS two-inductor boost converter with a resonant transition gate drive," IEEE Trans. Power Electronics, vol. 21, pp. 1253–1263, Sep. 2006.

19. W. C. P. De Aragão Filho and I. Barbi, "A comparison between two current-fed push-pull dc-dc converters—Analysis, design and experimen- tation," in Proc. INTELEC, 1996, pp. 313–320.

20. B. Yuan, X. Yang, X. Zeng, J. Duan, J. Zhai, and D. Li, "Analysis and design of a high step-up current-fed multiresonant dc-dc converter with